Supplement of Atmos. Chem. Phys., 26, 9721–9739, 2026
https://doi.org/10.5194/acp-26-9721-2026-supplement

Atmospheric Chemistry and Physics
Open Access
EGU

Supplement of

The importance of aerosol and droplet microphysics for the properties and life cycle of radiation fog in the Po Valley

Hao Ding et al.

Correspondence to: Hao Ding (hao.ding@misu.su.se) and Annica M. L. Ekman (annica.ekman@misu.su.se)

The supplementary information (SI) includes derivations of the droplet sedimentation scheme implemented in MIMICA model and aerosol hygroscopic growth scheme based on κ-Köhler theory; the initial meteorological conditions used in the reference simulation; and results from sensitivity experiments on surface forcing, microphysical process switches, and aerosol size distribution parameters. The SI sections are organized following the order of appearance in the main manuscript.

S1 Droplet sedimentation in MIMICA

For a droplet of radius r in the Stokes regime, the balance between buoyancy, viscous drag, and gravity can be expressed as:

$$\frac{4}{3}\pi r^3 \rho_f g + 6\pi\eta r v(r) = \frac{4}{3}\pi r^3 \rho_d g, \tag{S1}$$

where r is the droplet radius, ρ_f is the fluid density, η is the dynamic viscosity of the fluid, $v(r)$ is the terminal falling velocity, and ρ_d is the droplet density.
Solving for the terminal velocity yields:

$$v(r) = \frac{2}{9}\frac{g r^2(\rho_d - \rho_f)}{\eta}. \tag{S2}$$

In MIMICA, the droplet size distribution is described by a generalized gamma distribution:

$$n(d) = N\frac{\alpha}{\Gamma(\nu)}\lambda^{\alpha\nu} d^{\alpha\nu-1}\exp\left[-(\lambda d)^{\alpha}\right], \tag{S3}$$

where $n(d)$ is the number concentration of droplets of diameter d, N is the total droplet number concentration, λ is the slope parameter, α and ν are shape parameters, and Γ is the gamma function.
Considering that $v(r) \propto r^2$ in Eq. (S2), and based on the works of Bergot (2016) and Contreras Osorio et al. (2022), the bulk terminal velocity of droplets can be estimated by:

$$\langle v\rangle = C\langle r^2\rangle = C\frac{\langle r^5\rangle}{\langle r^3\rangle} = \frac{C}{\lambda^2}\frac{\Gamma\left(\nu+\frac{5}{\alpha}\right)}{\Gamma\left(\nu+\frac{3}{\alpha}\right)}, \tag{S4}$$

with

$$\lambda = \left[\frac{4}{3}\pi\frac{N\rho_d}{q\rho_f}\frac{\Gamma\left(\nu+\frac{3}{\alpha}\right)}{\Gamma(\nu)}\right]^{1/3}, \quad C = \frac{2}{9}\frac{g(\rho_d-\rho_f)}{\eta},$$

where q is the total liquid water content.

S2 FAIRARI measurement

Table S1. Overview of the main quantities and instruments from the FAIRARI campaign 2021/22, adapted from Neuberger et al. (2025b).

Measured quantity	**Height**	**Instrument**
Temperature, relative humidity	3.50 m	Weather transmitter WXT536, Vaisala, Finland
Wind vector, updraft velocity	5.55 m	Ultrasonic Anemometer, uSonic-3 Omni, Metek GmbH, Germany
Visibility	3.35 m	Visibility sensor 6400, Belfort Instrument, USA
Droplet number size distribution (300 nm-60 μm)	3.70 m	Ground-based Fog and Aerosol Spectrometer (GFAS), Droplet Measurement Techn., USA
Aerosol number size distribution (13.3 nm-792 nm)	8.15 m	Differential Mobility Particle Sizer (DMPS), Self-built, Karlsson et al. (2022)
Aerosol chemical component mass concentration	4.35 m	Soot Particle Aerosol Mass Spectrometer (SP-AMS), Aerodyne Research Inc., USA, Onasch et al. (2012)

S3 κ-Köhler theory

The κ-Köhler theory is employed to describe the hygroscopic growth and activation of aerosols. In this approach, the chemical property of the aerosol mixture (κ) is represented as a volume-fraction-weighted average of the hygroscopicity parameters (κ_i) of the individual species (Stokes and Robinson, 1966; Ranjan et al., 2025). The relationship between the wet particle diameter ($D_{p,\mathrm{wet}}$), dry particle diameter ($D_{p,\mathrm{dry}}$), and fractional ambient relative humidity (RH) is given by the implicit Köhler equation (Köhler, 1936; Petters and Kreidenweis, 2007):

$$S(D_{p,\mathrm{wet}}) = \frac{D_{p,\mathrm{wet}}^3 - D_{p,\mathrm{dry}}^3}{D_{p,\mathrm{wet}}^3 - D_{p,\mathrm{dry}}^3(1-\kappa)} \exp\left(\frac{4\sigma_{s/a} M_w}{RT\rho_w D_{p,\mathrm{wet}}}\right) = \mathrm{RH}, \tag{S5}$$

where $S(D_{p,\mathrm{wet}})$ denotes the saturation ratio, $\sigma_{s/a}$ the surface tension of the solution–air interface (0.0728 N m^{-1}), M_w the molar mass of water (0.018 kg mol^{-1}), R the universal gas constant (8.314 J mol^{-1} K^{-1}), T the temperature, and ρ_w the density of water (1000 kg m^{-3}).

The growth factor (GF) is defined as the ratio of wet to dry particle diameters:

$$\mathrm{GF} = \frac{D_{p,\mathrm{wet}}}{D_{p,\mathrm{dry}}}. \tag{S6}$$

Equation (S5) can be rewritten in terms of GF:

$$\mathrm{RH} = \frac{GF^3 - 1}{GF^3 - (1-\kappa)} \exp\left(\frac{4\sigma_{s/a} M_w}{RT\rho_w\, GF\, D_{p,\mathrm{dry}}}\right). \tag{S7}$$

Equation (S7) can be solved numerically to obtain prognostic GF in MIMICA, and the effect of aerosol hygroscopic growth on the water vapor budget Q_v is expressed as:

$$\Delta Q_v = (N_a - N_c)\frac{\pi}{6} D_{p,\mathrm{dry}}^3 \left(\mathrm{GF}^3 - 1\right)\rho_w, \tag{S8}$$

where N_a and N_c denote the number concentrations of total and activated aerosol particles, respectively.

S4 Initial meteorological conditions

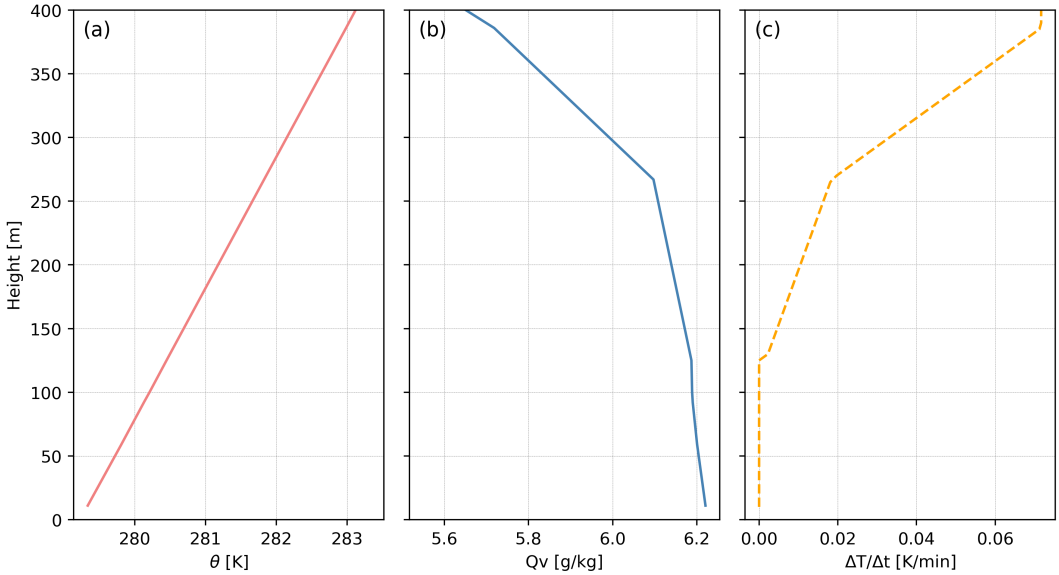

Figure S1. Initial vertical profiles of (a) potential temperature θ, (b) water vapor mixing ratio Q_v, (c) warm advection with the temperature change rate $\Delta T/\Delta t$ at 21:30-22:30 on 18 February 2022 in the reference simulation.

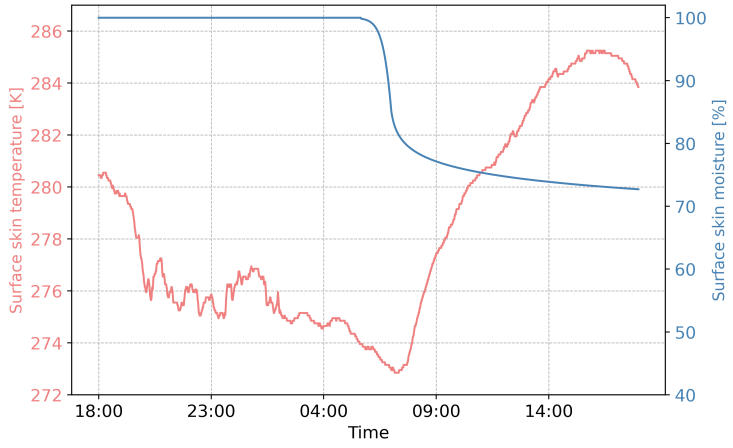

Figure S2. Surface skin temperature and moisture forcing on 18-19 February 2022 in the reference simulation.

S5 The role of implemented processes

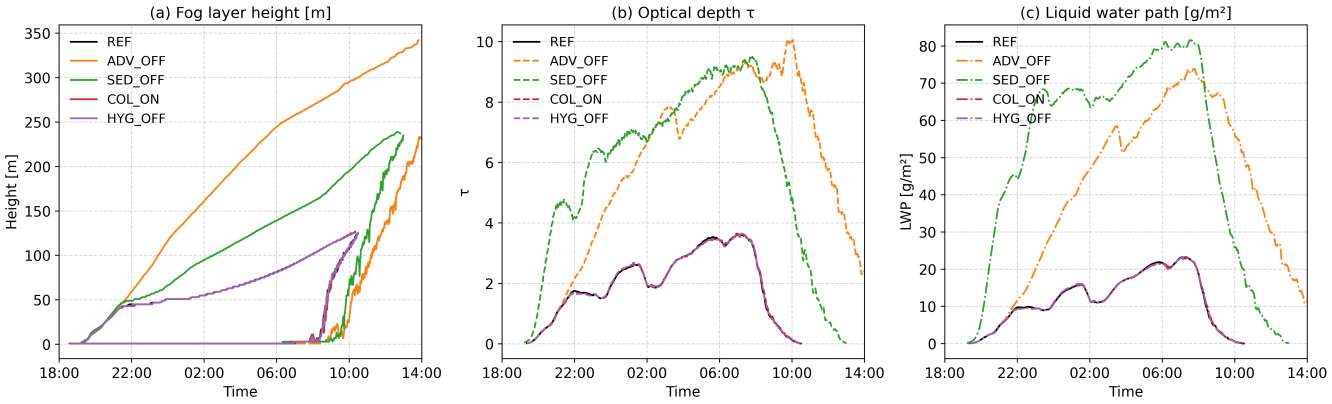

Figure S3. Vertical fog properties: (a) fog layer height, (b) optical thickness, and (c) liquid water path in the reference case (REF) and in tests with: advection off (ADV_OFF), droplet sedimentation off (SED_OFF), collision–coalescence on (COL_ON), and aerosol hygroscopic growth off (HYG_OFF).

S6 The importance of surface forcing

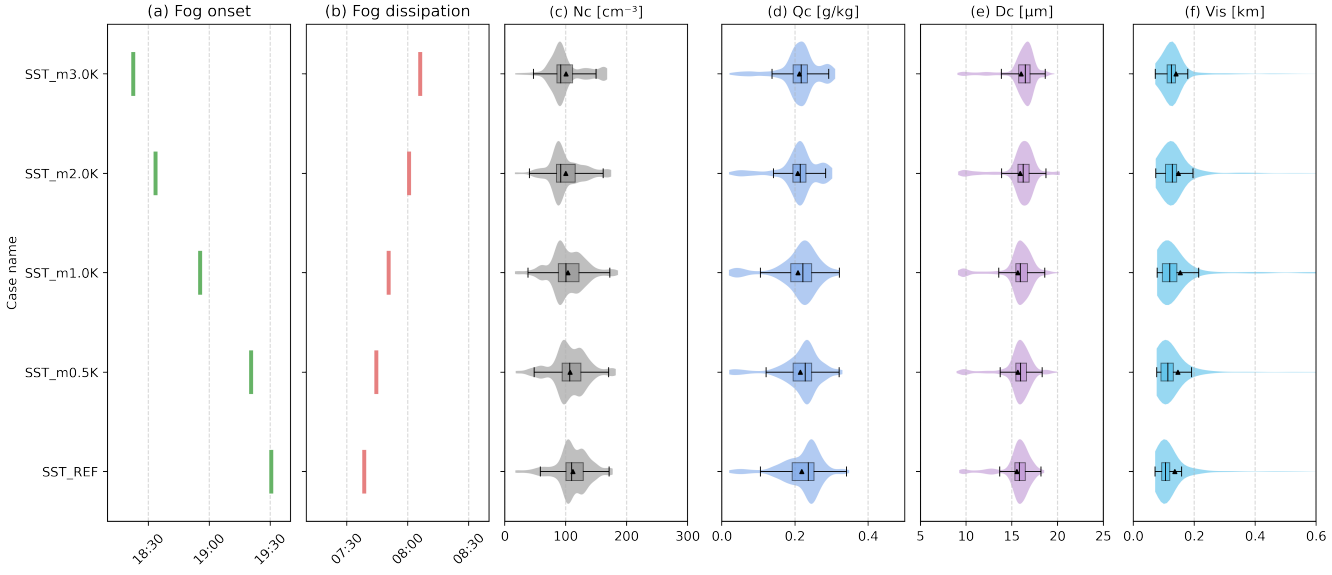

Figure S4. Statistical near-surface fog properties in the SFC_SST experiments (see Sect. 3.1): (a) fog onset time, (b) fog dissipation time, (c) droplet number concentration Nc, (d) liquid water mixing ratio Qc, (e) mean droplet diameter Dc and (f) visibility Vis. Both activated and hydrated particles are counted in droplet category. SST_mδTK denotes simulations where the surface skin temperature is reduced by δT K relative to the reference simulation. The boxes represent the 25$^{\text{th}}$–75$^{\text{th}}$ percentiles, whiskers the 5$^{\text{th}}$–95$^{\text{th}}$ percentiles, the solid line the median, and the black triangle the mean. Shaded areas illustrate the distribution of values.

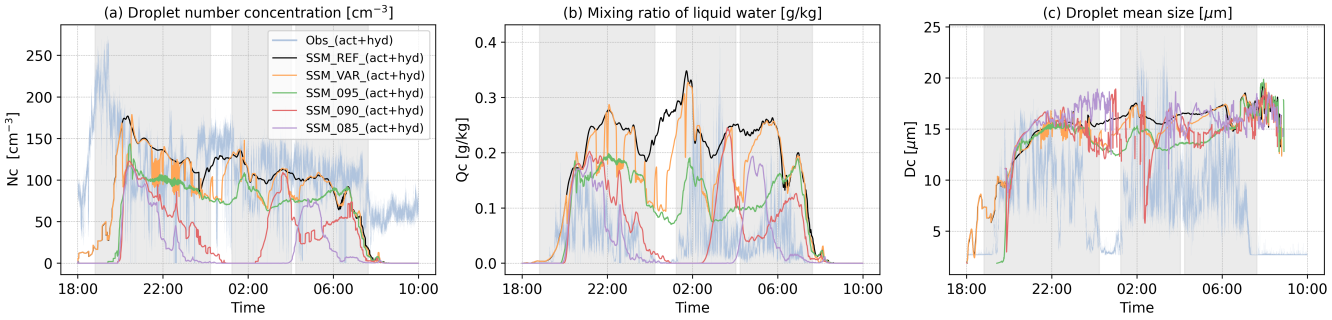

Figure S5. Time series of near-surface properties in the SFC_SSM experiments (see Sect. 3.1): (a) droplet number concentration, (b) liquid water mixing ratio and (c) droplet mean diameter. The shaded gray areas indicate fog periods identified from the observation.

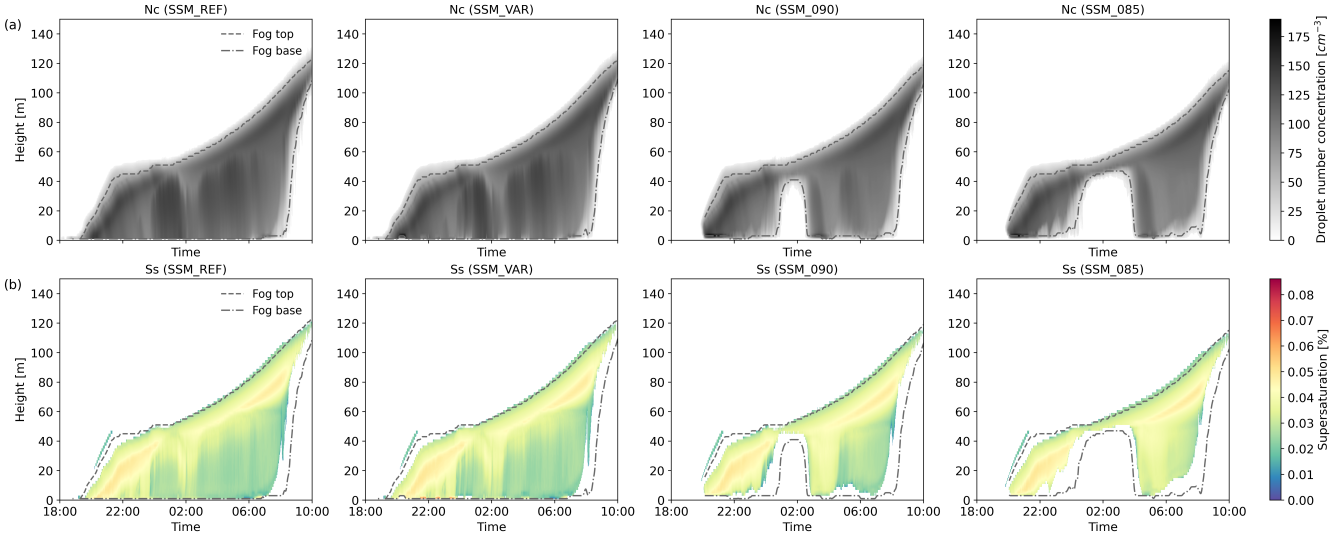

Figure S6. Time-height cross-sections of horizontally averaged fog properties in the SFC_SSM experiments (see Sect. 3.1): (a) droplet number concentration and panel (b) supersaturation.

S7 The importance of aerosol size distribution

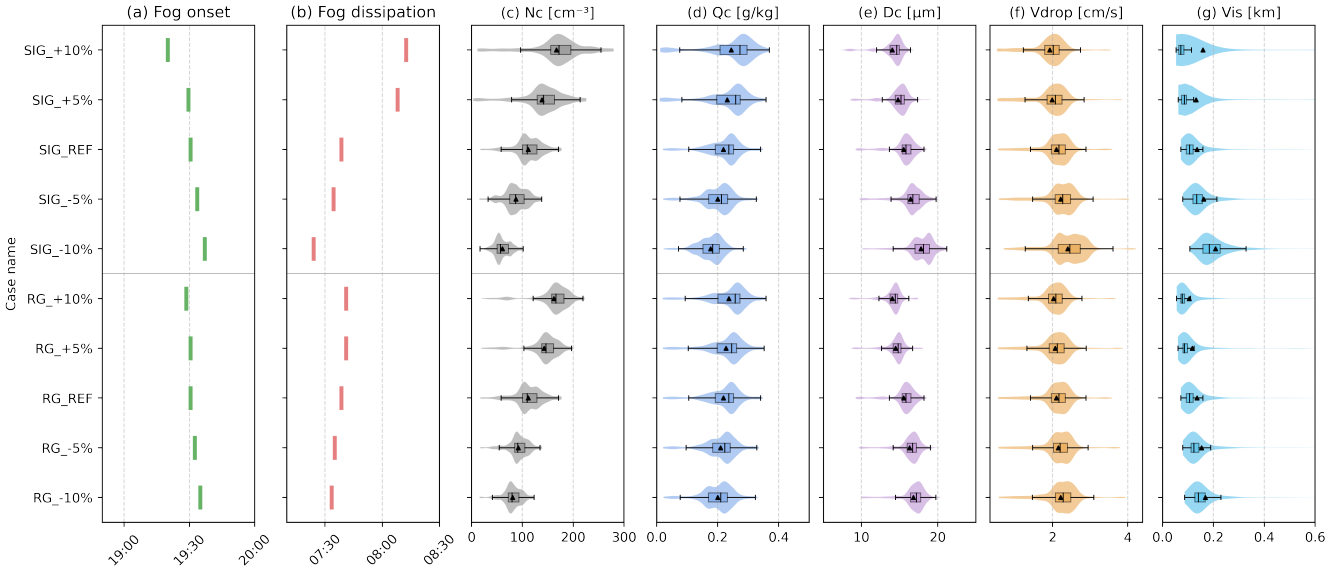

Figure S7. Statistical near-surface fog properties in AERO_RG and AERO_SIG experiments (see Sect. 2.4.1): (a) fog onset time, (b) fog dissipation time, (c) droplet number concentration Nc, (d) liquid water mixing ratio Qc, (e) mean droplet diameter Dc, (f) droplet terminal velocity Vdrop and (g) visbility Vis. Both activated and hydrated particles are counted in droplet category. The boxes represent the 25th–75th percentiles, whiskers the 5th–95th percentiles, the solid line the median, and the black triangle the mean. Shaded areas illustrate the distribution of values.

References

Bergot, T.: Large-eddy simulation study of the dissipation of radiation fog, Quarterly Journal of the Royal Meteorological Society, 142, 1029–1040, https://doi.org/10.1002/qj.2706, 2016.

Contreras Osorio, S., Martín Pérez, D., Ivarsson, K.-I., Nielsen, K. P., de Rooy, W. C., Gleeson, E., and McAufield, E.: Impact of the Microphysics in HARMONIE-AROME on Fog, Atmosphere, 13, 2127, https://doi.org/10.3390/atmos13122127, 2022.

Karlsson, L., Baccarini, A., Duplessis, P., Baumgardner, D., Brooks, I. M., Chang, R. Y., Dada, L., Dällenbach, K. R., Heikkinen, L., Krejci, R., Leaitch, W. R., Leck, C., Partridge, D. G., Salter, M. E., Wernli, H., Wheeler, M. J., Schmale, J., and Zieger, P.: Physical and chemical properties of cloud droplet residuals and aerosol particles during the Arctic Ocean 2018 expedition, Journal of Geophysical Research: Atmospheres, 127, e2021JD036 383, https://doi.org/10.1029/2021jd036383, 2022.

Köhler, H.: The nucleus in and the growth of hygroscopic droplets, Transactions of the Faraday Society, 32, 1152–1161, https://doi.org/10.1039/TF9363201152, 1936.

Neuberger, A., Decesari, S., Aktypis, A., Andersen, H., Baumgardner, D., Bianchi, F., Busetto, M., Cai, J., Cermak, J., Dipu, S., Ekman, A. M. L., Fuzzi, S., Gramlich, Y., Haslett, S. L., Heikkinen, L., Joutsensaari, J., Kaltsonoudis, C., Kangasluoma, J., Krejci, R., Lupi, A., Marinoni, A., Matrali, A., Mattsson, F., Mohr, C., Nenes, A., Paglione, M., Pandis, S. N., Patel, A., Riipinen, I., Rinaldi, M., Steimer, S. S., Stolzenburg, D., Sulo, J., Vasilakopoulou, C. N., and Zieger, P.: From Molecules to Droplets: The Fog and Aerosol Interaction Research Italy (FAIRARI) 2021/22 Campaign, Bulletin of the American Meteorological Society, 106, E23–E50, https://doi.org/10.1175/bams-d-23-0166.1, 2025b.

Onasch, T., Trimborn, A., Fortner, E., Jayne, J., Kok, G., Williams, L., Davidovits, P., and Worsnop, D.: Soot particle aerosol mass spectrometer: development, validation, and initial application, Aerosol Science and Technology, 46, 804–817, https://doi.org/10.1080/02786826.2012.663948, 2012.

Petters, M. and Kreidenweis, S.: A single parameter representation of hygroscopic growth and cloud condensation nucleus activity, Atmospheric Chemistry and Physics, 7, 1961–1971, https://doi.org/10.5194/acp-7-1961-2007, 2007.

Ranjan, R., Heikkinen, L., Ahonen, L. R., Luoma, K., Bowen, P., Petäjä, T., Ekman, A. M. L., Partridge, D. G., and Riipinen, I.: Optimizing CCN predictions through inferred modal aerosol composition – a boreal forest case study, EGUsphere, 2025, 1–35, https://doi.org/10.5194/egusphere-2025-1602, 2025.

Stokes, R. H. and Robinson, R. A.: Interactions in Aqueous Nonelectrolyte Solutions. I. Solute-Solvent Equilibria, The Journal of Physical Chemistry, 70, 2126–2131, https://doi.org/10.1021/j100879a010, 1966.